VNU Journal of Science, Earth Sciences 24 (2008) 79-86

Numerical study of long wave runup on a conical island

Phung Dang Hieu*

Center for Marine and Ocean-Atmosphere Interaction Research

Received 5 January 2008; received in revised form 10 July 2008

Abstract. A numerical model based on the 2D shallow water equations was developed using the Finite Volume Method. The model was applied to the study of long wave propagation and runup on a conical island. The simulated results by the model were compared with published experimental data and analyzed to understand more about the interaction processes between the long waves and conical island in terms of water profile and wave runup height. The results of the study confirmed the effects of edge waves on the runup height at the lee side of the island.

Keywords: Conical island; Runup; Finite volume method; Shallow water model.

1. Introduction

Simulation of two-dimensional evolution and runup of long waves on a sloping beach is a classical problem of hydrodynamics. It is usually related with the calculation of coastal effects of long waves such as tide and tsunami. Many researchers have contributed significantly efforts to the development of models capable of solving the problem. Notable studies can be mentioned. Shuto and Goto (1978) developed a numerical model based on finite difference method (FDM) on a staggered scheme [9]. Hibbert and Peregrine (1979) [2] proposed a model solving the shallow water equation in the conservation form using the Lax-Wendroff scheme and allowing for possible calculation of wave breaking. However, their model had not been capable to calculate wave runup and obtain physically realistic solutions. Subsequently, Kobayashi et al. (1987, 1989, 1990, 1992) [3, 4, 5, 6] refined the model for practical use, by adding dissipation terms in the finite-difference equations, what is now the most popular method for solving the shallow water equations. Liu et al. (1995) [7] modeled the runup of solitary wave on a circular island by FDM. Titov and Synolakis (1995, 1998) [11, 12] proposed models to calculate long wave runup on a sloping beach and circular island using FDM. Wei et al. (2006) [13] developed a model based on the shallow water equations using the finite volume method to simulate solitary waves runup on a sloping beach and a circular island. Simulated results obtained by Wei et al. agreed notably with laboratory experimental data [13].

Memorable tsunami in Indonesia and Japan caused millions of dollars in damages and killed thousands of people. On December 12, 1992, a 7.5-magnitude earthquake off

* Tel.: 84-914365198.
E-mail: phungdanghieu@vkttv.edu.vn

Flores Island, Indonesia, killed nearly 2500 people and washed away entire villages (Briggs et al., 1995) [1]. On Jully 12, 1993, a 7.8-magnitude earthquake off Okushiri Island, Japan, triggered a devastating tsunami with recorded runup as high as 30 m. This tsunami resulted in larger property damage than any 1992 tsunamis, and it completely inundated an village with overland flow. Estimated property damage was 600 million US dollars. Recently, the happened at December 26, 2004 Sumatra-Andaman tsunami-earthquake in the Indian Ocean with 9.3-magnitude and an epicenter off the west coast of Sumatra, Indonesia had killed more than 225,000 people in eleven countries and resulted in more than 1,100,000 people homeless. Inundation of coastal areas was created by waves up to 30 meters in height. This was the ninth-deadliest natural disaster in modern history. Indonesia, Sri Lanka, India, Thailand, and Myanmar were hardest hit.

Field surveys of tsunami damage on both Babi and Okushiri Islands showed unexpectedly large runup heights, especially on the back or lee side of the islands, respectively to the incident tsunami direction. During the Flores Island event, two villages located on the southern side of the circular Babi Island, whose diameter is approximately 2 km, were washed away by the tsunami attacking from the north. Similar phenomena occurred on the pear-shaped Okushiri Island, which is approximately 20 km long and 10 km wide (Liu et al., 1995) [7].

In this study, the interaction of long waves and a conical island is investigated using a numerical model based on the shallow water equation and finite volume method. The study is to simulate the processes of wave propagation and runup on the island in order to understand more the runup phenomena on conical islands. Supporting to the simulated results by the model, the experimental data proposed by Briggs el al. (1995) [1] were used.

2. Numerical model

2.1. Governing equation

The present study considers two-dimensional (2D) depth-integrated shallow water equations in the Cartesian coordinate system (x, y). The conservation form of the non-linear shallow water equations is written as [13]:

$$\frac{\partial \mathbf{U}}{\partial t} + \frac{\partial \mathbf{F}}{\partial x} + \frac{\partial \mathbf{G}}{\partial y} = \mathbf{S} \tag{1}$$

where $\mathbf{U}$ is the vector of conserved variables; $\mathbf{F}$, $\mathbf{G}$ is the flux vectors, respectively, in the x and y directions; and $\mathbf{S}$ is the source term. The explicit form of these vectors is explained as follows:

$$\mathbf{U} = \begin{bmatrix} H \\ Hu \\ Hv \end{bmatrix}, \ \mathbf{F} = \begin{bmatrix} Hu \\ Hu^2 + \frac{1}{2}gH^2 \\ Huv \end{bmatrix},$$

$$\mathbf{G} = \begin{bmatrix} Hv \\ Huv \\ Hv^2 + \frac{1}{2}gH^2 \end{bmatrix}, \ \mathbf{S} = \begin{bmatrix} 0 \\ gH\frac{\partial h}{\partial x} - \frac{\tau_x}{\rho} \\ gH\frac{\partial h}{\partial y} - \frac{\tau_y}{\rho} \end{bmatrix} \tag{2}$$

where g : gravitational acceleration; ρ : water density; h : still water depth; H : total water depth, $H = h + \eta$ in which $\eta(x, y, t)$ is the displacement of water surface from the still water level; τ_x, τ_y : bottom shear stress given by

$$\tau_x = \rho C_f u\sqrt{u^2 + v^2},$$

$$\tau_y = \rho C_f v\sqrt{u^2 + v^2}, \ C_f = \frac{gn^2}{H^{1/3}} \tag{3}$$

where n : Manning coefficient for the surface roughness.

2.2. Numerical scheme

The finite volume formulation imposes conservation laws in a control volume. Integration of Eq. (1) over a cell with the application of the Green's theorem, gives:

$$\int_\Omega \frac{\partial \mathbf{U}}{\partial t} d\Omega + \int_\Gamma (\mathbf{F}n_x + \mathbf{G}n_y) d\Gamma = \int_\Omega \mathbf{S} d\Omega, \quad (4)$$

where Ω: cell domain; Γ: boundary of Ω; (n_x, n_y): normal outward vector of the boundary.

Taking time integration of Eq. (4) over duration Δt from t_1 to t_2, we have

$$\int_\Omega \mathbf{U}(x,y,t_2) d\Omega - \int_\Omega \mathbf{U}(x,y,t_1) d\Omega + \int_{t_1}^{t_2} dt \int_\Gamma (\mathbf{F}n_x + \mathbf{G}n_y) d\Gamma = \int_{t_1}^{t_2} dt \int_\Omega \mathbf{S} d\Omega \quad (5)$$

The present model uses uniform cells with dimension Δx, Δy, thus, the integrated governing equations (5) with a time step Δt can be approximated with a half time step average for the interface fluxes and source term to become:

$$\mathbf{U}_{i,j}^{k+1} = \mathbf{U}_{i,j}^{k} - \frac{\Delta t}{\Delta x}\left[\mathbf{F}_{i+1/2,j}^{k+1/2} - \mathbf{F}_{i-1/2,j}^{k+1/2}\right] - \frac{\Delta t}{\Delta y}\left[\mathbf{G}_{i,j+1/2}^{k+1/2} - \mathbf{G}_{i,j-1/2}^{k+1/2}\right] + \Delta t \mathbf{S}_{i,j}^{k+1/2} \quad (6)$$

where i, j are indices at the cell center; k denotes the current time step; the half indices $i+1/2$, $i-1/2$ and $j+1/2$, $j-1/2$ indicate the cell interfaces; and $k+1/2$ denotes the average within a time step between k and $k+1$. Note that, in Eq. (6) the variables $\mathbf{U}$ and source term $\mathbf{S}$ are cell-averaged values (we use this meaning from now on).

To solve Eq. (6), we need to estimate the numerical fluxes $\mathbf{F}_{i+1/2,j}^{k+1/2}$, $\mathbf{F}_{i-1/2,j}^{k+1/2}$ and $\mathbf{G}_{i,j+1/2}^{k+1/2}$, $\mathbf{G}_{i,j-1/2}^{k+1/2}$ at the cell interfaces. In this study, we use the Godunov-type scheme for this purpose. According to the Godunov-type scheme, the numerical fluxes at a cell interface could be obtained by solving a local Riemann problem at the interface.

Since direct solutions are not available for two or three dimensional Riemann problems, the present model uses the second-order splitting scheme of Strang (1968) [10] to separate Eq. (6) into two one-dimensional equations, which are integrated sequentially as:

$$\mathbf{U}_{i,j}^{k+1} = X^{\Delta t/2} Y^{\Delta t} X^{\Delta t/2} \mathbf{U}_{i,j}^{k} \quad (7)$$

where X and Y denote the integration operators in the x and y directions, respectively. The equation in the x direction is first integrated over a half time step and this is followed by integration of a full time step in the y direction. These are expressed as:

$$\mathbf{U}_{i,j}^{(k+1/2)^*} = \mathbf{U}_{i,j}^{k} - \frac{\Delta t}{2\Delta x}\left[\mathbf{F}_{i+1/2,j}^{k+1/4} - \mathbf{F}_{i-1/2,j}^{k+1/4}\right] + \frac{\Delta t}{2}(\mathbf{S}_x)_{i,j}^{k+1/4} \quad (8)$$

$$\mathbf{U}_{i,j}^{(k+1)^*} = \mathbf{U}_{i,j}^{(k+1/2)^*} - \frac{\Delta t}{\Delta y}\left[\mathbf{G}_{i,j+1/2}^{k+1/2} - \mathbf{G}_{i,j-1/2}^{k+1/2}\right] + \Delta t(\mathbf{S}_y)_{i,j}^{k+1/2} \quad (9)$$

where the asterisk (*) indicates partial solutions at the respective time increments within a time step and $\mathbf{S}_x$, $\mathbf{S}_y$ are the source terms in the x direction and y directions. Integration in the x direction over the remaining half time step advances the solution to the next time step:

$$\mathbf{U}_{i,j}^{k+1} = \mathbf{U}_{i,j}^{(k+1)^*} - \frac{\Delta t}{2\Delta x}\left[\mathbf{F}_{i+1/2,j}^{k+3/4} - \mathbf{F}_{i-1/2,j}^{k+3/4}\right] + \frac{\Delta t}{2}(\mathbf{S}_x)_{i,j}^{k+3/4} \quad (10)$$

The partial solutions $\mathbf{U}_{i,j}^{k}$, $\mathbf{U}_{i,j}^{(k+1/2)^*}$ and $\mathbf{U}_{i,j}^{(k+1)^*}$, provide the interface flux terms in equations (8), (9) and (10) through a Riemann solver in one-dimensional problems. In this study, we use the HLL approximate Riemann solver for the estimation of numerical fluxes. For the wet and dry cell treatment, we use the

minimum wet depth, the cell is assumed to be dry if its water depth less than the minimum wet depth (in this study we choose minimum wet depth of 10^{-5} m).

3. Simulation results and discussion

3.1. Experimental condition

A numerical experiment is carried out for the condition similar to the experiment done by Briggs et al. (1995) [1]. In this experiment, there was a conical island setup in a wave basin having the dimension of 30 m wide and 25 m long. The conical island has the shape of a truncated cone with diameters of 7.2 m at the base and 2.2 m at the crest. The island is 0.625 m high and has a side slope of 1:4. The surface of the island and basin has a smooth concrete finish. There is absorbing materials placed at the four sidewalls to reduce wave reflection. The water depth is $h = 0.32$ m. A solitary wave with the height of $A/h = 0.2$ was generated for the experimental observation. Fig. 1 shows the sketch of the experiment and wave gauge location for water surface measurement. Five time-series data of water surface elevation were collected for the comparison.

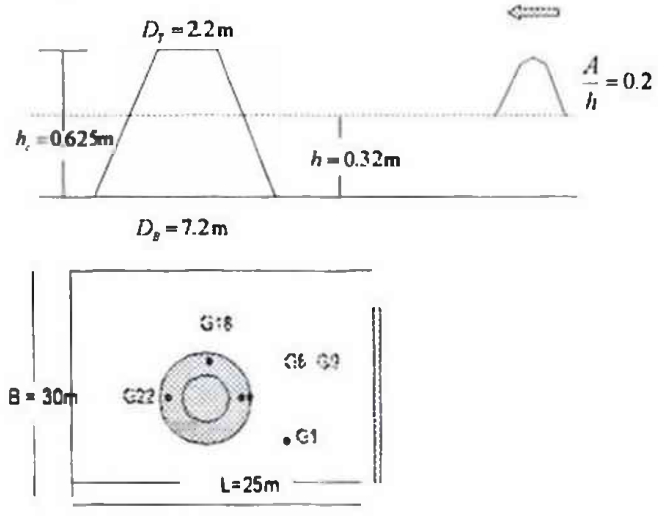

Fig. 1. Sketch of the experiment.

In Fig. 1, the wave gauge G1 is setup for the measurement of the incident waves; wave gauges G6 and G9 are for the waves in the shoaling area; and the wave gauges G16 and G22 are respectively, for waves on the right side and lee side of the island. The locations of the five wave gauges are given in Table 1 in relation with the center of the island.

Table 1. Location of wave gauges

Gauge num.	$x - x_c$ (m)	$y - y_c$ (m)
G1	9.00	2.25
G6	3.60	0.00
G9	2.60	0.00
G16	0.00	2.58
G22	-2.60	0.00

(x_c, y_c): coordinate of the center of the island

3.2. Numerical simulation and discussion

In the numerical simulation, a computation domain is setup similar to the experiment. The mesh is regular with grid size of 0.1 m in both x and y directions. At four sides of the computation domain, radiation boundary conditions are used in order to allow waves to go freely through the side boundary. A solitary wave is generated as the initial condition at a line parallel with the y direction, and located at the distance of 12.96 m from the center of the island. The Manning coefficient is set to be constant $n = 0.016$. The initial solitary wave is created by using the following equation:

$$\eta(x) = A\,\mathrm{sech}^2\left[\sqrt{\frac{3A}{4h^3}}(x - x_s)\right] \tag{11}$$

$$u(x) = \eta(x)\sqrt{\frac{g}{h}} \tag{12}$$

where x_s is the center of the solitary wave.

The numerical results of water surface elevation at five wave-gauge locations and runup height on the island are recorded for

validation of the simulation. Fig. 2a shows the time profile of water surface elevation at the wave gauge G1. In this figure, it is seen that the incident solitary wave simulated by the model agrees very well with the experimental data. This gives us a confidence in comparison of time series of water surface elevation at other locations in the computation domain, as well as in comparison of wave runup on the island.

In the Fig. 2b and 2c, at the wave gauges G6 and G9, it is seen that the solitary wave is well simulated on the shoaling region, the wave comes to the location after about 4 seconds from the initial time. At first, the numerical results and experimental data agree very well, after that, there are some discrepancy appeared. This deflection can be explained due to the reflection from the side boundaries in the experiment done by Briggs et al, much larger than that in the simulation.

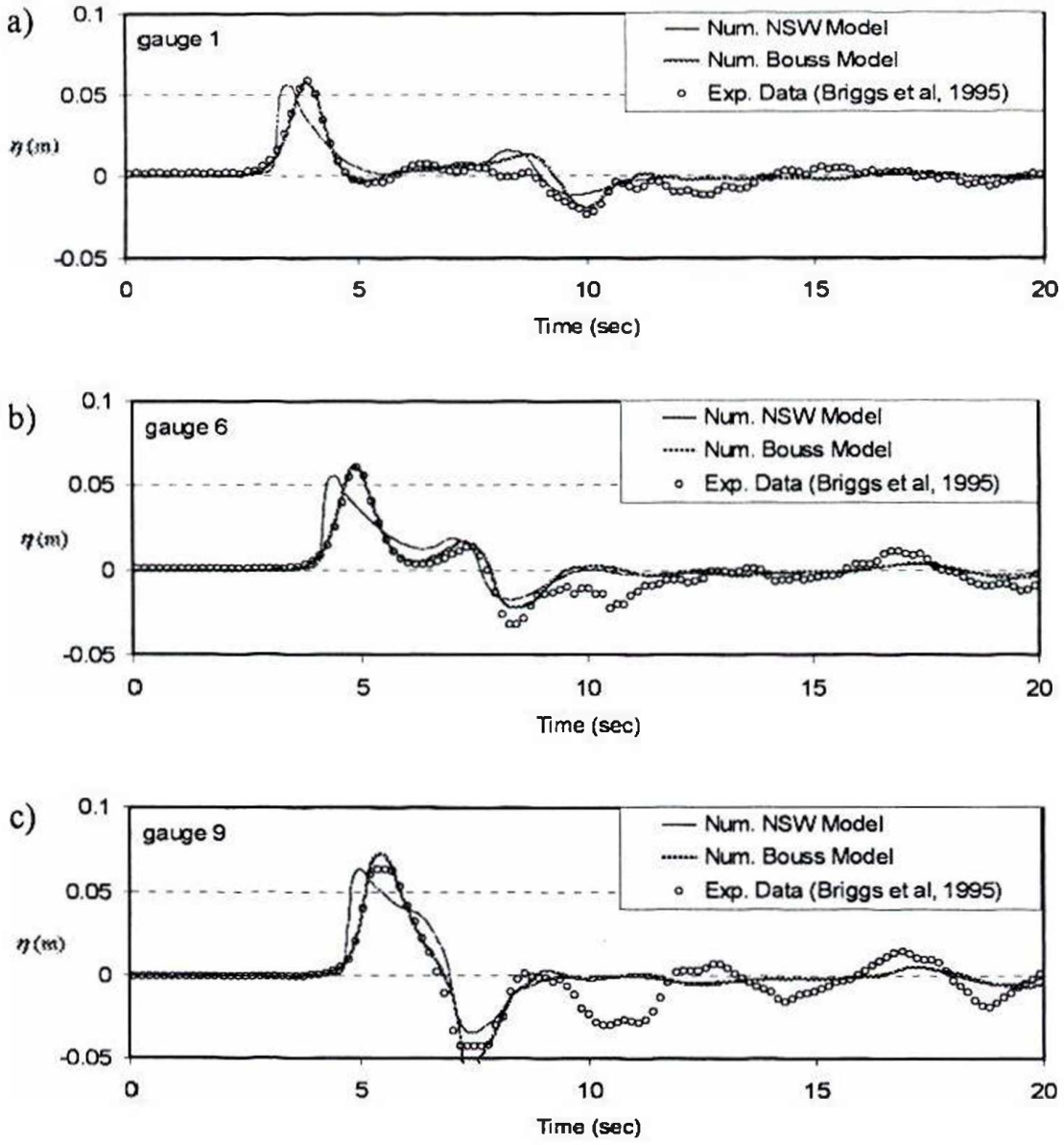

Fig. 2. Comparison of water surface elevation at locations G1, G6, G9: solid thin line: simulated by common shallow water equation; solid thick line: simulated by adding Boussinesq term to the shallow water equation.

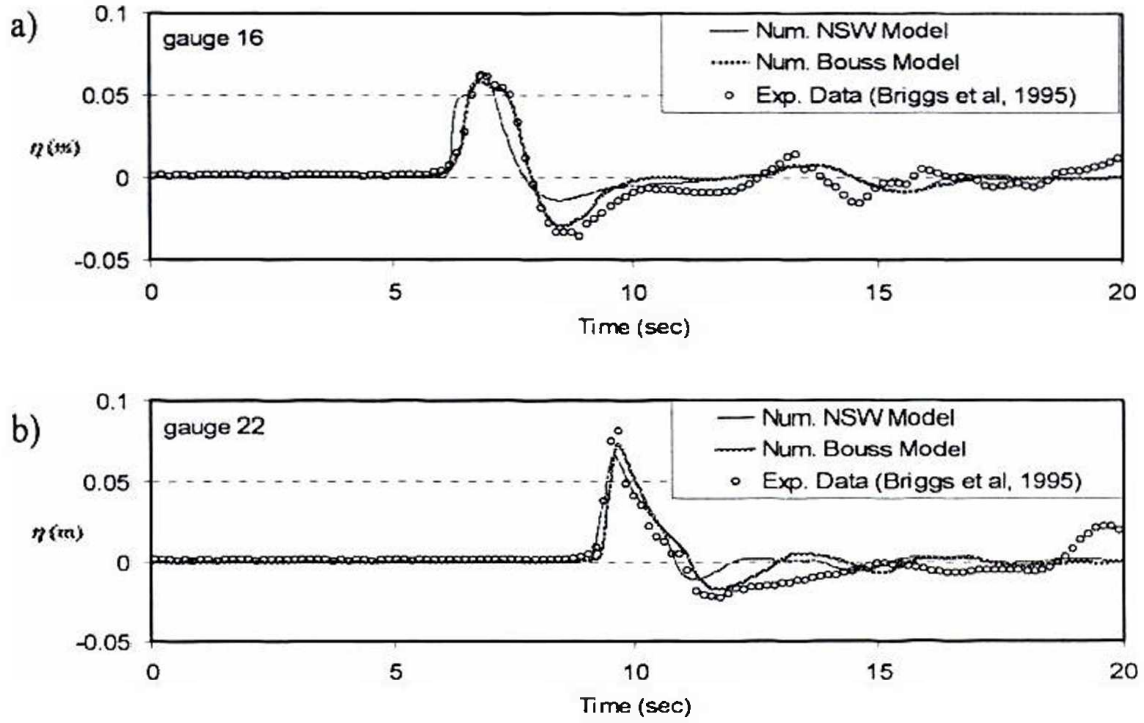

Fig. 3. Comparison of water surface elevation at locations G16 and G22: solid thin line: simulated by common shallow water equation; solid thick line: simulated by adding Boussinesq term to the shallow water equation.

It can be confirmed from the figure that, the numerical results very soon become stable having non-fluctuation when the wave goes freely out of the experiment domain. Inversely, the experimental data have a long tail of disturbance and could not be calm after 20s (see Fig. 2, at wave gauges G6 and G9; and Fig 3, at wave gauges G16 and G22). This fluctuation is due to the wave energy dissipation not enough at the sides of the experiment basin. However, the form and height of the arriving solitary wave at all locations are well matched between experimental and numerical results. This is very important to allow later comparison of wave runup on the island.

From Fig. 2 and Fig. 3, it is also seen that, the wave height at the lee side (gauge G22, Fig. 3b) of the island is still very high in comparison with the height at the front side (gauge G6, G9, Fig. 2b, 2c) of the island, and much bigger than that at the right side (gauge G16, Fig. 3a) of the island. These results give us a confidence in confirming that the wave height at lee side of an circular island can be large also. In Fig. 2 and Fig. 3, two sets of numerical results are plotted. One is simulated by the common non-linear shallow water equation (NSW), and the other is simulated by adding the Boussinesq dispersion term [8] into the NSW. From the figures, it is confirmed that the model using the Boussinesq approximation can give simulated results much better than the common NSW based model. Thus, for the practical purpose of simulation non-linear long wave problem, the Boussinesq approximation terms should be considered.

Fig. 4 shows the snapshot of water surface displacement on the computation domain. From the figure, we can see that, after the solitary wave comes to the island, the wave refraction appears due to the variation of water depth. Behind the island, the edge waves come from two sides of the island due to waves bending around the island and matching together at

the leeside of the island. Then, they form an area of very high wave rushing up to the lee side coast of the island. This mechanism can be explained for the unexpectedly large runup heights on the leeside of the Babi and Okushiri Islands due to the tsunami.

Fig. 5 is the comparison of wave runup around the island, between numerical simulation and experiment. The horizontal axis in the figure indicates the angle between the line drawing from the center of the island to the point of runup measurement and the y direction. The angle of 0 degree means that the measuring point is at the right side of the island and on the line through the center of the island and normal to the incident wave direction (i.e. parallel to the y direction). It is shown from the figure that, the runup is highest at the foreside of the island, the maximum simulated runup height is somewhat less than experimental data. At the leeside of the island, there is an area with runup higher than both sides of the island. The numerical results of runup height in this area are also smaller than experimental data. These might be due to the fact that the computational mesh not fine enough to capture highly non-linear interactions of edge waves at the leeside. In overall, the numerical model can simulate well the runup height at many locations around the island. Especially, the tendency of the runup variation and runup location are well simulated by the present numerical model. This means that, the model developed in this study has potential features to apply to the study of practical problems related with long waves, such as inundation of tsunami on coastal areas.

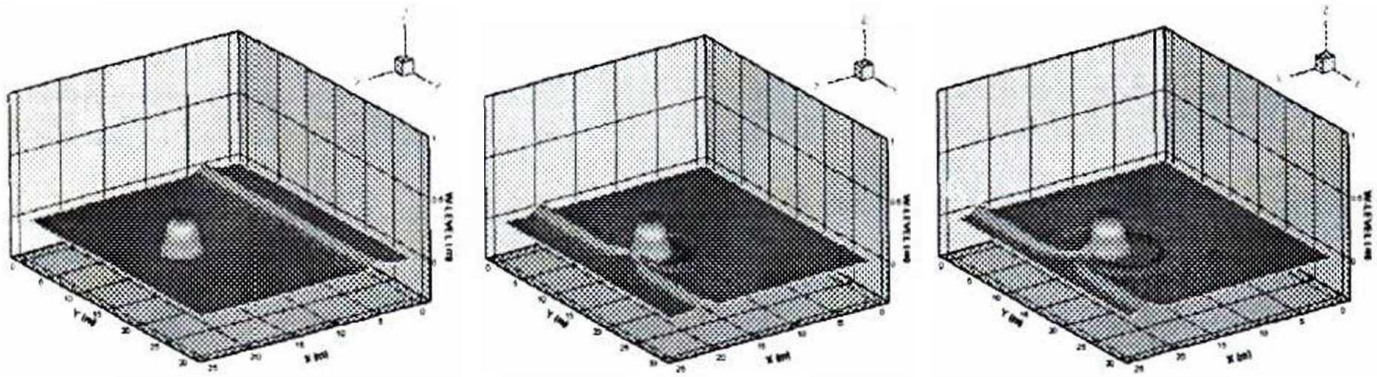

Fig. 4. Snapshots of the water surface displacement due to the solitary wave.

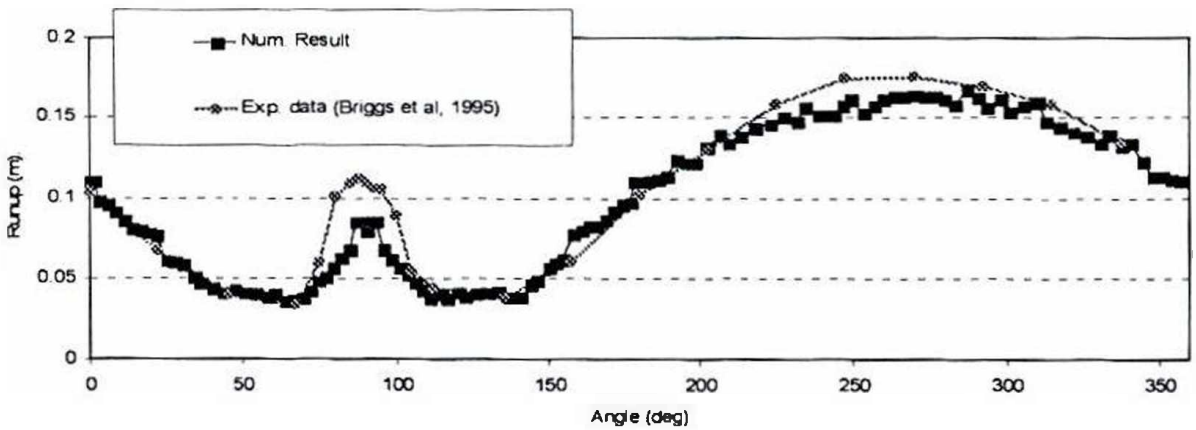

Fig. 5. Runup of water around the island due to the solitary wave (270 deg.: at foreside in the normal direction of wave propagation; 90 deg.: at the leeside of the island; 0 deg.: at the right side of the island; and 180 deg.: at the left side of the island).

4. Conclusions

A 2D numerical model based on the shallow water equation has been successfully developed for the simulation of long wave propagation, deformation and runup on the conical island. The numerical results simulated by NSW model and by Boussinesq model revealed that by adding Boussinesq terms to the NSW model, simulated results of long wave propagation and deformation can be significantly improved. Therefore, it is worth to mention that Boussinesq approximation should be considered in a practical problem related with long waves. The model also has potential features to apply to the study of practical problems related to long waves, such as inundation of tsunami on coastal areas.

Simulated results in this study also confirm that the area behind an island can be attacked by big waves coming from the opposite side of the island due to non-linear interaction of edge waves resulted from refraction processes.

Acknowledgments

This paper was completed within the framework of Fundamental Research Project 304006 funded by Vietnam Ministry of Science and Technology.

References

[1] M.J. Briggs et al, Laboratory experiments of tsunami runup on a circular island, *Pure Applied Geophys.* 144 (1995) 569.

[2] S. Hibbert, D.H. Peregrine, Surf and runup on a beach: a uniform bore, *Journal of Fluid Mechanics* 95 (1979) 323.

[3] N. Kobayashi, A.K. Otta, I. Roy, Wave reflection and runup on rough slopes, *J. Waterway, Port, Coastal and Ocean Engineering* 113 (1987) 282.

[4] N. Kobayashi, G.S. DeSilva, K.D. Wattson, Wave transformation and swash oscillations on gentle and steep slopes, *Journal of Geophysics Research* 94 (1989) 951.

[5] N. Kobayashi, D.T. Cox, A. Wurjanto, Irregular wave reflection and runup on rough impermeable slopes, *Journal of Waterway, Port, Coastal and Ocean Engineering* 116 (1990) 708.

[6] N. Kobayashi, A. Wurjanto, Irregular wave setup and runup on beaches, *Journal Waterway, Port, Coastal and Ocean Engineering* 118 (1992) 368.

[7] P.L-F Liu et al, Runup of solitary wave on a circular island, *Journal of Fluid Mechanics* 302 (1995) 259.

[8] P.A. Madsen, O.R. Sorensen, H.A. Schaffer, Surf zone dynamics simulated by Boussinesq type model, Part I: Model description and cross-shore motion of regular waves, *Coastal Engineering* 32 (1997) 255.

[9] N. Shuto, C. Goto, Numerical simulation of tsunami runup, *Coastal Engineering Journal-Japan* 21 (1978) 13.

[10] G. Strang, On the construction and comparison of difference schemes, *SIAM* (Soc. Int. Appl. Math.) *Journal of Numerical Analysis* 5 (1968) 506.

[11] V.V. Titov, C.E. Synolakis, Modeling of breaking and non-breaking long-wave evolution and runup using VTCS-2, *Journal of Waterway, Port, Coastal and Ocean Engineering* 121 (1995) 308.

[12] V.V. Titov, C.E. Synolakis, Numerical modeling of tidal wave runup, *Journal of Waterway, Port, Coastal and Ocean Engineering* 124 (1998) 157.

[13] Y. Wei, X.Z. Mao, K.F. Cheung, Well-balanced finite-volume model for long-wave runup. *Journal of Waterway, Port, Coastal and Ocean Engineering* 132 (2006) 114.